

## First-Order Localized-Electron $\rightleftharpoons$ Collective-Electron Transition in $\text{LaCoO}_3$

P. M. RACCAH AND J. B. GOODENOUGH

*Lincoln Laboratory,\* Massachusetts Institute of Technology, Lexington, Massachusetts*

(Received 1 August 1966)

Precision x-ray measurements of the motions of the atoms in  $\text{LaCoO}_3$  every  $50^\circ\text{C}$  from room temperature to  $1000^\circ\text{C}$  indicate that the crystal space group is  $R\bar{3}c$  below  $375^\circ\text{C}$  and  $R\bar{3}$  above  $375^\circ\text{C}$ . In the symmetry  $R\bar{3}$  there are two distinguishable octahedral cobalt positions,  $\text{Co}_I$  having larger crystalline fields than  $\text{Co}_{II}$ . Since high- and low-spin cobalt ions are simultaneously present, this indicates preferential long-range ordering of low-spin cobalt at  $\text{Co}_I$  sites, and of high-spin cobalt at  $\text{Co}_{II}$  sites for  $T > 375^\circ\text{C}$ . Calorimetric data show a first-order transition at  $T_t = 937^\circ\text{C}$  and a higher order transition in the temperature interval  $125 < T < 375^\circ\text{C}$ , which is also manifest in a large Debye-Waller factor in this interval and in a plateau in the curve of reciprocal susceptibility versus temperature. At about  $650^\circ\text{C}$  there is some evidence, from differential thermal-analysis data, of another higher order transition. The electrical conductivity increases with increasing temperature below  $650^\circ\text{C}$ , but much more rapidly in the interval  $125 < T < 650^\circ\text{C}$  than below  $125^\circ\text{C}$ . It is nearly temperature-independent in the interval  $650 < T < 937^\circ\text{C}$  and is continuous through the first-order transition. However, above  $937^\circ\text{C}$  the resistivity increases with temperature as in a metal. The space group remains  $R\bar{3}$  and the pseudocubic cell edge is continuous through the first-order phase change, but the rhombohedral angle drops abruptly from  $60.4^\circ$  to  $60^\circ$  and the  $\text{La}^{3+}$  ions are shifted discontinuously along the  $c$  axis toward a  $\text{Co}_I$  ion. Similar  $\text{La}^{3+}$ -ion displacements occur in the temperature interval  $400 < T < 650^\circ\text{C}$ . The Debye-Waller factor decreases by an order of magnitude on going to the high-temperature phase. It is pointed out that crystal-field and band theory should describe two different thermodynamic states of electrons: localized and collective. The data are interpreted to indicate (1) that the first-order phase change at  $T_t = 937^\circ\text{C}$  is a localized-electron  $\rightleftharpoons$  collective-electron phase change for electrons in orbitals of  $e_g$  symmetry, higher temperatures introducing a Fermi surface and partial disproportionation between high- and low-spin cations at  $\text{Co}_{II}$  and  $\text{Co}_I$  positions; (2) that the number of charge carriers is constant through the transition, because the number of localized charge carriers is saturated below  $T_t$  and just above  $T_t$  the bandwidth of the collective-electron states is  $\Delta e < kT_t$ ; (3) that the mobilities of the charge carriers are also continuous through the transition, the activation energy for a localized-electron hop becoming  $\ll kT$  at  $T \leq 937^\circ\text{C}$ ; (4) that the higher-order transition in the interval  $125 < T < 375^\circ\text{C}$  represents a region of short-range order, the ordered phase occurring at higher temperatures where the populations of high- and low-spin cobalt ions approach one another; and (5) that exciton transfer is an important mechanism in  $\text{LaCoO}_3$ .

### I. INTRODUCTION

#### A. Motivation

COMPARISON<sup>1</sup> of the physical properties of transition-metal oxides with the perovskite or  $\text{ReO}_3$  structure, which is illustrated in Fig. 1, has revealed that if, given a localized  $d$ -electron model, the predicted cationic spin is  $S \leq \frac{1}{2}$ , then metallic conductivity and Pauli paramagnetism is found, indicating that the outer  $d$  electrons are better described by band theory. However, if  $S \geq 2$ , the compounds have an atomic moment that is well described by crystal-field theory and an interatomic cation-anion-cation magnetic-exchange interaction that is well described by superexchange theory. In addition, Jahn-Teller distortions are found where there are four outer  $d$  electrons and  $S = 2$ . Thus for  $S \geq 2$ , the outer  $d$  electrons clearly appear to be localized. These facts suggest that transition-metal oxides with the perovskite structure offer the possibility of studying the properties of electrons in solids as the conditions for stabilization of localized versus collective (crystal-field versus band)  $d$  electrons are varied continuously.

In a previous study,<sup>2</sup> it was noted that  $\text{LaCoO}_3$  undergoes a first-order phase change at  $937^\circ\text{C}$  ( $1210^\circ\text{K}$ ). It was also noted in this and other studies<sup>3-7</sup> that magnetic-susceptibility-versus-temperature data indicate that for the octahedral-site, trivalent cobalt ions the energy difference between the diamagnetic ( $S = 0$ ), low-spin state  $^1A_1$  and the paramagnetic ( $S = 2$ ), high-spin state  $^5T_2$  is

$$E_{3+} - E_{III} \leq 0.08 \text{ eV}, \quad (1)$$

where the low-spin ions, designated  $\text{Co}^{III}$  in this paper, are more stable than the high-spin  $\text{Co}^{3+}$  ions. This finding appears to confirm the suggestion made some years ago<sup>8</sup> that  $E_{3+} \approx E_{III}$  in the entire system  $\text{La}_{1-x}\text{Sr}_x\text{CoO}_3$ . The simultaneous existence of low-spin ( $S = 0$ ) and high-spin ( $S = 2$ ) cobalt ions immediately suggests the following possibilities: (1) High-spin and low-spin cobalt

<sup>2</sup> J. B. Goodenough and P. M. Racciah, *J. Appl. Phys. Suppl.* **36**, 1031 (1965).

<sup>3</sup> R. R. Heikes, R. C. Miller, and R. Mazelsky, *Physica* **30**, 1600 (1964).

<sup>4</sup> G. H. Jonker, *J. Appl. Phys.* **37**, 1424 (1966).

<sup>5</sup> G. Blasse (quoted in Ref. 4).

<sup>6</sup> C. S. Naiman, R. Gilmore, B. DiBartolo, A. Linz, and R. Santoro, *J. Appl. Phys.* **36**, 879 (1965).

<sup>7</sup> N. Menyuk, K. Dwight, and P. M. Racciah, *J. Phys. Chem. Solids* (to be published).

<sup>8</sup> J. B. Goodenough, *J. Phys. Chem. Solids* **6**, 287 (1958).

\* Operated with support from the U. S. Air Force.

<sup>1</sup> J. B. Goodenough, *J. Appl. Phys.* **37**, 1415 (1966).

ions may order preferentially on alternate (111) cobalt planes, as suggested<sup>8</sup> earlier for the system  $\text{La}_{1-x}\text{Sr}_x\text{CoO}_3$ , and (2) the first-order phase change at 937°C may correspond to a localized-electron  $\rightleftharpoons$  collective-electron transition for the  $d$  electrons of  $e_g$  symmetry. The present study was motivated by a desire to investigate experimentally these two possibilities.

## B. Background Considerations

### 1. Cationic Order

Octahedral-site crystal fields split one-electron local  $d$  levels into threefold-degenerate  $t_{2g}$  and twofold-degenerate  $e_g$  levels by an energy  $\Delta_{cf}$ , and the intra-atomic exchange energy stabilizes a splitting of states of different spin by an energy  $\Delta_{ex}$ . Low-spin ions have  $\Delta_{cf} > \Delta_{ex}$ , so that the outer-electron configuration is  $t_{2g}^6 e_g^0$ ; high-spin ions have  $\Delta_{cf} < \Delta_{ex}$  and therefore  $t_{2g}^4 e_g^2$ . It follows that ordering of high- and low-spin cobalt ions onto alternate (111) planes would be manifest by a cooperative motion of the oxygen ions that produces shorter Co-O distances, and hence larger  $\Delta_{cf}$ , at one family of (111) cobalt planes and larger Co-O distances at the other, as illustrated schematically by sublattices  $\text{Co}_I$  and  $\text{Co}_{II}$  in Fig. 2.

### 2. Localized versus Collective Electrons

Covalent mixing of anionic wave functions into the cationic  $d$ -wave functions does not destroy the symmetry classification  $e_g$  and  $t_{2g}$ . The crystal-field,  $d$ -like orbitals of an octahedral, cobalt-oxygen complex have the form<sup>1</sup>

$$\Psi_e = N_\sigma (f_e + \lambda_\sigma \varphi_\sigma) \quad (2)$$

and

$$\Psi_t = N_\pi (f_t + \lambda_\pi \varphi_\pi),$$

where  $f_e$  and  $f_t$  are the cationic orbitals of  $e_g$  and  $t_{2g}$  symmetry,  $N_\sigma$  and  $N_\pi$  are normalization constants, and the covalent-mixing parameters  $\lambda_\sigma$  and  $\lambda_\pi$  are a measure of the covalent mixing of the cationic orbitals with the anionic orbitals  $\varphi_\sigma$  and  $\varphi_\pi$  of the six near-neighbor anions that either  $\sigma$  bond or  $\pi$  bond with the cations. In the perovskite structure (see Fig. 1) there are only three possible overlap integrals for the orbitals  $\Psi_e$  and  $\Psi_t$  on neighboring cations:

$$\begin{aligned} \Delta_{ee} &\equiv (\Psi_{t1}, \Psi_{t3}), \\ \Delta^{\sigma_{eae}} &\equiv (\Psi_{e1}, \Psi_{e2}) = N_\sigma^2 \lambda_\sigma^2, \\ \Delta^{\pi_{eae}} &\equiv (\Psi_{t1}, \Psi_{t2}) = N_\pi^2 [\lambda_\pi^2 + 2\lambda_\pi (f_t, \varphi_\pi)], \end{aligned} \quad (3)$$

where cations labeled 1 and 3 are on opposite sides of a cube (or pseudocube) face and 1 and 2 are near-neighbors on a cube (or pseudocube) edge with an anion intermediary. From experiments on the monoxides, sesquioxides, and dioxides it has been possible to show<sup>9</sup>

<sup>9</sup> J. B. Goodenough, in *Progress in Solid State Chemistry*, edited by H. Reiss (Pergamon Press, Inc., New York, 1967), Vol. 5.

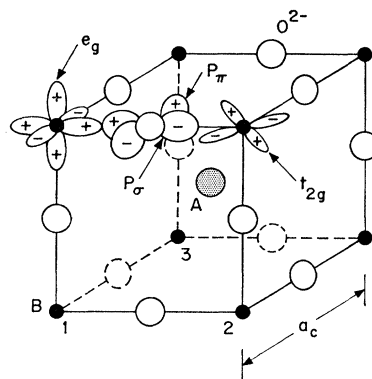


FIG. 1. Pseudocubic (or cubic) cell of the perovskite structure. Chemical formula is  $\text{ABO}_3$ , where B is a transition-metal cation and A is a large, electropositive cation having no outer  $d$  electrons. Representative orbitals are also indicated: a  $p_\sigma$  and a  $p_\pi$  anion orbital, orbitals of  $e_g$  symmetry ( $d_{x^2-y^2}$ ,  $d_{z^2}$ ), and the  $d_{xy}$  orbital of the orbitals of  $t_{2g}$  symmetry ( $d_{xy}$ ,  $d_{yz}$ ,  $d_{zx}$ ). B cations marked 1, 2, and 3 have overlap integrals  $\Delta_{eae}^\pi < \Delta_{eae}^\sigma$  between 1 and 2, 1 and 3; and an overlap integral  $\Delta_{ee}^\sigma$  between 2 and 3, where the integrals are defined by Eq. (3).

that the distance across a cube face  $R \approx 5.5 \text{ \AA}$  is so large that  $\Delta_{ee}$  is negligibly small. This means that the magnitudes of the overlap integrals  $\Delta^{\pi_{eae}}$  and  $\Delta^{\sigma_{eae}}$ , where by symmetry  $\Delta^{\pi_{eae}} < \Delta^{\sigma_{eae}}$ , determine the character of the outer  $d$  electrons. If these integrals are large enough, it is appropriate to construct collective-electron (band) orbitals out of the various orbitals  $\Psi_e$  and  $\Psi_t$ : Such orbitals, which are antibonding with respect to the anions, are designated  $\sigma^*$ - and  $\pi^*$ -band orbitals, respectively, so as to differentiate them from localized orbitals, which do not reflect the translational symmetry of a periodic, crystalline potential. On the other hand, if the overlap integrals are small enough, the  $d$  electrons are localized to discrete cationic sites, and the

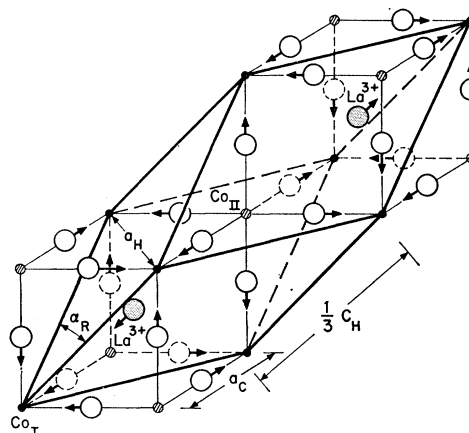


FIG. 2. Rhombohedral unit cell of  $\text{LaCoO}_3$ . Only those components of the anion and  $\text{La}^{3+}$ -ion displacements found in space group  $R\bar{3}$  are shown that introduce different crystalline fields at sublattices  $\text{Co}_I$  and  $\text{Co}_{II}$ . These displacements are not present in the space group  $R\bar{3}c$ , in which only anion displacements perpendicular to a Co-Co axis occur. Hexagonal parameters  $a_H$ ,  $c_H$ , a pseudocubic parameter  $a_c$ , and the rhombohedral angle  $\alpha_R$  are also defined.

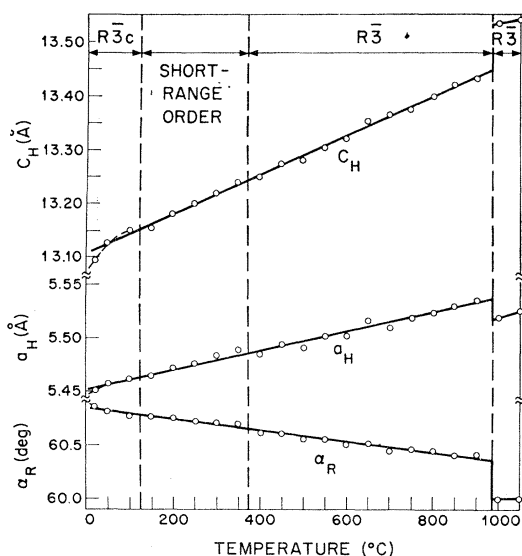


FIG. 3. Hexagonal-cell lattice parameters and rhombohedral angle  $\alpha_R$  as a function of temperature.

crystal-field orbitals  $\Psi_e$  and  $\Psi_t$  are coupled to similar orbitals on neighboring cations via superexchange interactions, which have magnitudes proportional to  $(\Delta_{cac})^2 \sim \lambda^4$ . Conceptually, it is possible to define a critical overlap integral  $\Delta_c$  such that the outer  $d$  electrons are localized, crystal-field electrons if  $\Delta_{cac} < \Delta_c$  and collective, band electrons if  $\Delta_{cac} > \Delta_c$ . Further, experiments indicate<sup>1</sup> (see above) that  $\Delta_{cac}^{\sigma} < \Delta_c$  if  $S \geq 2$  and  $\Delta_{cac}^{\sigma} > \Delta_{cac}^{\pi} \geq \Delta_c$  if  $S \leq \frac{1}{2}$ . This suggests that the intra-atomic-exchange potential, which contracts the radial extension of the atomic wave functions (Hartree-Fock versus Hartree wave functions), reduces the overlap integrals sufficiently to change the electronic character from collective to localized on converting from low- to high-spin cobalt. [Thermal excitation of low-spin cobalt is not to a state having a  $\sigma^*$ -band electron, where the  $\sigma^*$  band is separated from the  $t_{2g}^6$  level by  $\sim 1$  eV, because the high-spin state is energetically closer, according to Eq. (1).<sup>10</sup>] In a system in which low- and high-spin cobalt are simultaneously present, there is the possibility that  $\langle \Delta_{cac}^{\sigma} \rangle \approx \Delta_c$  and, therefore, that a localized-electron  $\rightleftharpoons$  collective-electron transition may occur.

With an integral number of  $d$  electrons per transition-metal cation, a localized-electron configuration corresponds to a "Fermi solid" having the  $d$ -electron fermions ordered at discrete transition-metal atom sites, and a collective-electron configuration corresponds to a "Fermi gas" moving in a periodic potential. These represent two electronic phases, and it is reasonable to anticipate that a first-order phase change is required to change from one to the other. Such a first-order phase change would signal a sharply defined  $\Delta_c$ . If the entropy of the

<sup>10</sup> In  $\text{LaRhO}_3$  the high-spin state is energetically more removed, and the physical properties are characteristic of a broad-band semiconductor.

collective-electron phase is sufficiently larger than that of the localized-electron phase and if the thermal reduction of the overlap integrals (via thermal expansion of the lattice) is small enough, then it might be possible to observe a first-order localized-electron  $\rightleftharpoons$  collective-electron transition as a function of temperature.

### C. Strategy

The present study is primarily structural, but it is supplemented by differential thermal analysis (DTA) and calorimetry and by a check of the transport and magnetic properties previously reported in the literature. The problem was to devise a method of refining powder, x-ray-intensity data so as to obtain precision measurements of the individual atomic positions. Such measurements unambiguously reveal whether there is preferential ordering of high- and low-spin cations and simultaneously indicate how the overlap integrals are changing with temperature. The measurements clearly reveal preferential ordering of high- and low-spin cobalt ions on alternate (111) cobalt planes in the temperature interval  $375 < T \leq 1000^\circ\text{C}$  and appear to provide the first experimental demonstration of a first-order localized-electron  $\rightleftharpoons$  collective-electron transition. Given this interpretation of the transition, the data also indicate that those physical properties, such as electron mobility, that are independent of the existence of a Fermi surface vary continuously through the transition.

## II. EXPERIMENTAL

### A. Sample Preparation

Since  $\text{La}_2\text{O}_3$  picks up water and  $\text{CO}_2$  from the atmosphere, weighing of stoichiometric quantities of the oxides is unreliable. A more accurate La/Co ratio was obtained by starting with oxalates whose water of hydration had been determined from thermogravimetric measurements.

The mixture of oxalates was decomposed by slow heating to  $600^\circ\text{C}$ . After decomposition, the powder was pressed into pellets and the temperature raised to values varying from 1000 to  $1200^\circ\text{C}$ . Two days were long enough to give a single-phase material having the x-ray pattern characteristic of a rhombohedral perovskite. However, the magnetic susceptibility exhibited an anomaly below  $77^\circ\text{K}$  that suggested the possibility of chemical inhomogeneities. Although repeated mechanical grinding and refiring appeared to eliminate part of the magnetic anomaly, a small ( $\sim 1\%$ ) moment of ferromagnetic (or ferrimagnetic) second phase remained.<sup>7</sup> Nevertheless, where checks were made, these inhomogeneities appeared to have no measurable influence on the high-temperature calorimetric and structural properties reported in this paper.

The La/Co ratio of the final material was analyzed by x-ray fluorescence, and it was always unity within

experimental error. The state of oxidation of the cobalt was determined from weight loss under hydrogen. No evidence of  $\text{Co}^{4+}$  was ever detected. However, this thermogravimetric measurement revealed that samples heated over  $1050^\circ\text{C}$  suffered a loss of oxygen, 1 to 5%  $\text{Co}^{2+}$  being present, so that the x-ray measurements were limited to temperatures  $T \leq 1000^\circ\text{C}$ .

### B. Calorimetry

A differential thermal analysis was performed from room temperature to  $1200^\circ\text{C}$ . It revealed an endothermic, first-order transition at  $937^\circ\text{C}$  and higher order transitions in the interval  $125 < T < 375^\circ\text{C}$  and at about  $650^\circ\text{C}$ . The lowest of these transitions was investigated more precisely by dynamic calorimetry and the center of the transition appeared to be at about  $230^\circ\text{C}$ .

### C. X-Ray Diffraction

#### 1. Method

Powder x-ray data were collected every fifty degrees from room temperature to  $1000^\circ\text{C}$  under copper  $K\alpha$  radiation. The data were collected on a GE XRD-5 diffractometer with the aid of a temp-press camera. At each temperature, the positions of the Bragg peaks and accurate, integrated relative intensities were measured. The method for deducing accurate atomic positions from the raw data has been described elsewhere.<sup>11,12</sup> The usual crystallographic discrepancy index  $R$  is different for each plausible space group, and the most probable structure corresponds to the lowest  $R$  value.

In order to study changes in atomic positions as a function of temperature, this criterion was applied to powder data. The feasibility of the method has been demonstrated for the spinel structure,<sup>12</sup> where checks with accurate neutron data were possible. It has also been demonstrated for form-factor studies for  $\text{MgO}$ <sup>13</sup> and  $\text{ZnSe}$ .<sup>14</sup> The fact that neutron data<sup>15</sup> were also available for the rhombohedral perovskite  $\text{LaAlO}_3$  permitted a further check, which also confirmed the accuracy of the method (see Appendix). Finally, it has been possible to show,<sup>16</sup> both by this x-ray technique and by thermogravimetric analysis, that lead ruthenate with defect pyrochlore structure has the chemical formula  $\text{Pb}_2\text{Ru}_2\text{O}_6$  rather than  $\text{Pb}_2\text{Ru}_2\text{O}_7$  and that the  $\text{Pb}^{2+}$  ions donate their two outer electrons to the anion vacancy, thus demonstrating that it is possible to observe the oxygen ions in the presence of the heavy

<sup>11</sup> P. M. Raccach and P. H. Trent, M.I.T. Lincoln Laboratory Solid State Research Report No. 2, 1965, p. 33 (unpublished).

<sup>12</sup> P. M. Raccach, R. J. Bouchard, and A. Wold, *J. Appl. Phys.* **37**, 1436 (1966).

<sup>13</sup> P. M. Raccach and R. J. Arnott, *Phys. Rev.* **153**, 1028 (1967).

<sup>14</sup> P. M. Raccach, R. J. Arnott, and A. Wold, *Phys. Rev.* **148**, 904 (1966).

<sup>15</sup> C. DeRango, G. Tsoncaris, and C. Zelwar, *Compt. Rend.* **259**, 1537 (1964).

<sup>16</sup> J. M. Longo, P. M. Raccach, and J. B. Goodenough, *J. Chem. Phys.* (to be published).

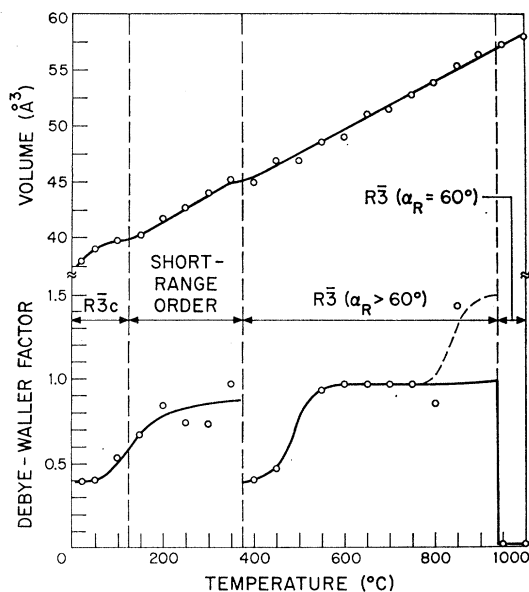


FIG. 4. Rhombohedral-cell volume and Debye-Waller factor as a function of temperature.

elements Pb and Ru. Table IV of the Appendix compares observed and calculated intensities for  $\text{LaCoO}_3$  at  $400^\circ\text{C}$ , which was a typical run.

#### 2. Symmetry Considerations

The rhombohedral perovskite cell contains two molecules, as shown in Fig. 2. So long as the transition-metal ion remains a center of inversion symmetry, three space groups are possible:  $R\bar{3}c$ ,  $R\bar{3}m$ , and  $R\bar{3}$ . In the space group  $R\bar{3}c$ , the two cobalt ions are not distinguishable, and the close-packed, oxygen-lanthanum (111) planes remain equidistant from neighboring (111) cobalt planes. In the space group  $R\bar{3}m$ , the two cobalt ions ( $\text{Co}_I$  and  $\text{Co}_{II}$ ) per unit cell are not equivalent; the oxygen and lanthanum (111) planes, which coincide in  $R\bar{3}c$  symmetry, are displaced independently along the  $c$  axis. These displacements are in pairs toward  $\text{Co}_I$  planes and away from  $\text{Co}_{II}$  planes, so that the crystal-field splitting  $\Delta_{e_f}$  is larger at a  $\text{Co}_I$  ion than at a  $\text{Co}_{II}$  ion. In the space group  $R\bar{3}$ , neither the  $c$ -axis glide nor the mirror symmetry is preserved, and the atomic displacements may be decomposed into an  $R\bar{3}c$  component and an  $R\bar{3}m$  component. A second-order transformation from  $R\bar{3}c$  symmetry to a symmetry having differentiated cobalt positions would, according to the Landau-Lifshitz theorem,<sup>17</sup> be to the symmetry  $R\bar{3}$ .

#### 3. Results

The lattice parameters, cell volume, La-Co and Co-O separations, and the Debye-Waller factors are displayed as a function of temperature in Figs. 3-6. Between room

<sup>17</sup> L. D. Landau and E. M. Lifshitz, *Statistical Physics*, translated by E. Peierls and R. F. Peierls (Pergamon Press, Inc., London, 1958), p. 439.

temperature and 100°C, the symmetry is apparently  $R\bar{3}c$ . Neutron-diffraction data have shown that this is also the most probable space group from liquid helium to room temperature.<sup>7</sup> Above 375°C, the oxygen (111) planes are definitely displaced so as to give two cobalt-oxygen distances, and the symmetry is reduced to  $R\bar{3}$ . Note that these oxygen displacements are large compared to the temperature variation of the Co-Co separation  $a_c$ .

In the interval  $400 < T < 650^\circ\text{C}$ , the reduced symmetry is also manifest by a motion of the lanthanum ions along the  $c$ -axis away from the near-neighbor  $\text{Co}_{\text{II}}$  ion towards the near-neighbor  $\text{Co}_{\text{I}}$  ion on this axis. The phase relationship in this temperature interval between the oxygen and lanthanum displacements parallel to the  $c$ -axis is believed to be real, the initiation of a lanthanum displacement coinciding with the maximum oxygen displacement parallel to the  $c$  axis and the termination of the lanthanum displacement coinciding with a minimum oxygen displacement parallel to the  $c$  axis. A similar static displacement of the lanthanum ions occurs discontinuously across the first-order-transition temperature  $T_t = 937^\circ\text{C}$ .

In the intervals  $125 \leq T < 375^\circ\text{C}$  and  $550 \leq T < 937^\circ\text{C}$ , the Debye-Waller factors are significantly larger than in the rest of the temperature range, which suggests either static short-range ordering or a temperature region of larger atomic vibrations. The fact that there is no long-range ordering of distinguishable cobalt ions below  $125^\circ\text{C}$  and that there is above  $375^\circ\text{C}$  indicates that, in the interval  $125 \leq T \leq 375^\circ\text{C}$ , the apparently large Debye-Waller factor associated with an  $R\bar{3}c$  symmetry assignment is due to short-range order. This is compatible with the observation of a higher-order transition in this interval. In the interval  $650 \leq T < 937^\circ\text{C}$ ,

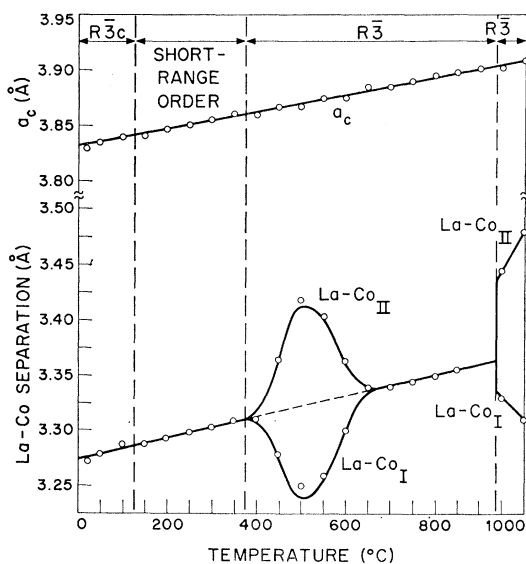


Fig. 5. Pseudocubic-cell edge  $a_c$  and  $\text{La-Co}_{\text{I}}$ ,  $\text{La-Co}_{\text{II}}$  separations as a function of temperature.

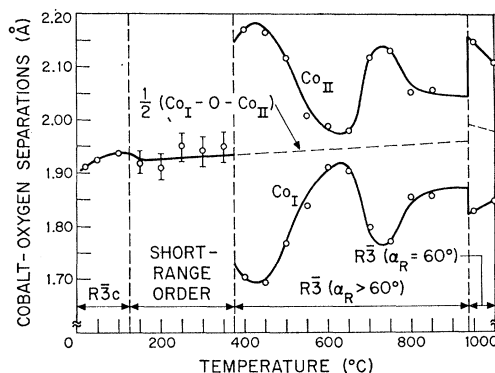


Fig. 6.  $\text{Co}_{\text{I}}\text{-O}$  and  $\text{Co}_{\text{II}}\text{-O}$  separations as a function of temperature.

on the other hand, the symmetry assignment  $R\bar{3}$  gives a significantly lower value for the discrepancy index  $R$  than the assignment  $R\bar{3}c$ , and large ionic vibrations rather than static short-range order appear to be required to account for the larger Debye-Waller factor.

As the temperature is increased across the transition temperature  $T_t = 937^\circ\text{C}$ , the rhombohedral angle  $\alpha_R$  decreases abruptly from  $60.4^\circ$  to  $60.0^\circ$ , which causes corresponding discontinuities in the hexagonal parameters  $a_H$  and  $c_H$ , but the pseudocubic cell edge  $a_c$  appears to vary continuously. Within experimental error, it was not possible to determine the discontinuous change in unit-cell volume, discontinuities in  $a_c$  and/or volume due to discontinuities in  $\alpha_R$  being extremely small. This is unusual for a first-order transition. Since the rate of change of the transition temperature with pressure is

$$dT_t/dP = T\Delta V/\Delta H,$$

where  $\Delta V$  is the volume change across the transition and  $\Delta H$  is the heat of transformation, an extremely small  $\Delta V$  relative to  $\Delta H$  implies that  $T_t$  is insensitive to pressure. This may account for our observation that several rare-earth cobaltates (R.E.) $\text{CoO}_3$ , which have different cell sizes due to different ionic radii, exhibit first-order phase changes at approximately the same  $T_t$ .

Although the rhombohedral angle becomes  $\alpha_R = 60.0^\circ$  in the high-temperature phase, the symmetry remains  $R\bar{3}$  because of the lanthanum- and oxygen-ion displacements. Below the transition, the anion displacements responsible for different  $\text{Co}_{\text{I}}\text{-O}$  and  $\text{Co}_{\text{II}}\text{-O}$  separations exhibit maxima near  $425^\circ\text{C}$  and  $725^\circ\text{C}$ , but in the interval  $650 < T < 937^\circ\text{C}$  there is no apparent displacement of the lanthanum ions from a body-center position of the pseudocubic cell. At  $937^\circ\text{C}$ , the oxygen-ion displacements exhibit a third maximum. However, it would appear that the  $\text{Co}_{\text{I}}\text{-O}$  and  $\text{Co}_{\text{II}}\text{-O}$  separations along any pseudocubic edge have only a small, discontinuous change at the transition temperature. (There is a small discontinuity in the  $\text{Co}_{\text{I}}\text{-O}-\text{Co}_{\text{II}}$  distance, even though the Co-Co separation  $a_c$  appears to be continuous, because of displacements of the anions perpendicular to the Co-Co axes in response to the lan-

TABLE I. Model of cobalt-ion configuration and  $d$ -electron character in  $\text{LaCoO}_3$  for various temperature intervals.  $\text{Co}^{2+}$ ,  $\text{Co}^{3+}$  indicates the high-spin state and  $\text{Co}^{\text{III}}$ ,  $\text{Co}^{\text{IV}}$  indicates the low-spin state.

Temperature Interval	Dominant cobalt-ion configuration <sup>a</sup>	$d$ electrons
$-273 < T < 125^\circ\text{C}$	Disorder $\text{Co}^{3+}$ among majority $\text{Co}^{\text{III}}$	Localized
$125 \leq T < 375^\circ\text{C}$	Short-range order of $\text{Co}^{3+}$ and $\text{Co}^{\text{III}}$	Localized
$375 \leq T < 937^\circ\text{C}$	Long-range order into $\text{Co}_\text{I}$ and $\text{Co}_\text{II}$	Localized
$375 \leq T < 400^\circ\text{C}$	(a) $\text{Co}_\text{I} = \text{Co}^{\text{III}}$ ; $\text{Co}_\text{II} = (1-x)\text{Co}^{3+} + \text{Co}^{\text{III}}$	
$400 < T < 500^\circ\text{C}$	(b) $\text{Co}_\text{I} = (1-y)\text{Co}^{\text{III}} + y\text{Co}^{2+}$ ; $\text{Co}_\text{II} = (1-x-y)\text{Co}^{3+} + x\text{Co}^{\text{III}} + y\text{Co}^{\text{IV}}$	
$500 \leq T < 650^\circ\text{C}$	(c) $\text{Co}_\text{I} = (1-y-z)\text{Co}^{\text{III}} + y\text{Co}^{2+} + z\text{Co}^{3+}$ ; $\text{Co}_\text{II} = (1-y-z)\text{Co}^{3+} + y\text{Co}^{\text{IV}} + z\text{Co}^{\text{III}}$	
$650 \leq T < 937^\circ\text{C}$	(d) $\text{Co}_\text{I} = (1-2\lambda-z)\text{Co}^{\text{III}} + \lambda(\text{Co}^{2+} + \text{Co}^{\text{IV}}) + z\text{Co}^{3+}$ ; $\text{Co}_\text{II} = (1-2\lambda-z)\text{Co}^{3+} + \lambda(\text{Co}^{\text{IV}} + \text{Co}^{2+}) + z\text{Co}^{\text{III}}$	
$937 < T \leq 1000^\circ\text{C}$	Long-range order: $\text{Co}_\text{I}(t_2\sigma^{8-x}\sigma^{*y})$ ; $\text{Co}_\text{II}(t_2\sigma^{4+x}\sigma^{*2-y})$ ; $x < y$	Collective

<sup>a</sup>  $x \rightarrow 0$  as increasing  $T \rightarrow \sim 500^\circ\text{C}$ .  $y$  increases from a small value at  $\sim 400^\circ\text{C}$  to a maximum at  $\sim 500^\circ\text{C}$  and decreases to a small value at  $\sim 600^\circ\text{C}$ .  $z$  increases from a small value at  $\sim 500^\circ\text{C}$  to a relatively large value for  $T \geq 650^\circ\text{C}$ .  $\lambda$  increases from a small value at  $\sim 650^\circ\text{C}$  to a large value just below  $T_t = 937^\circ\text{C}$ .

thanum-ion displacements.) On the other hand, there is a dramatic, discontinuous change in the Debye-Waller factor at  $937^\circ\text{C}$ .

#### D. Other Physical Properties

##### 1. Magnetic Susceptibility

At higher temperatures, the magnetic susceptibilities measured by various workers<sup>2-7</sup> are in essential agreement. The characteristic feature is a plateau in the reciprocal-susceptibility-versus-temperature curve in the temperature interval  $125 < T < 375^\circ\text{C}$ , as shown in Fig. 7. Such a plateau between two temperature regions exhibiting different slopes, corresponding to a lower  $\mu_{\text{eff}}$  in the low-temperature interval, has also been observed in the system  $\text{MnAs}_{1-x}\text{P}_x$  and identified with a variation in the populations of low- versus high-spin ions, the high-spin population being larger at higher temperatures.<sup>18</sup>

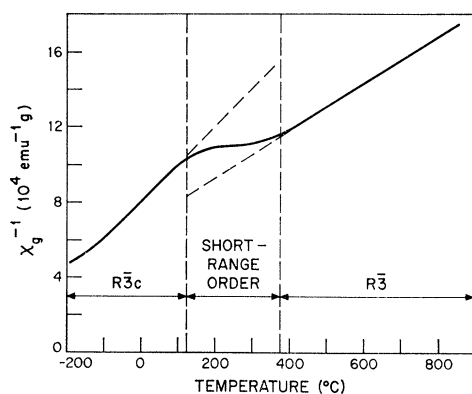


FIG. 7. Inverse magnetic susceptibility per gram as a function of temperature.

<sup>18</sup> J. B. Goodenough, D. H. Ridgley, and W. A. Newman, in *Proceedings of the International Conference on Magnetism, Nottingham, 1964* (Institute of Physics and The Physical Society, London, 1965), p. 542.

##### 2. Electrical Conductivity

Below  $125^\circ\text{C}$ ,  $\text{LaCoO}_3$  is a semiconductor with a conductivity given approximately by

$$\sigma = \sigma_0 \exp(-q/kT). \quad (4)$$

Above  $125^\circ\text{C}$ , the conductivity increases much more rapidly with increasing temperature, changing by over two orders of magnitude in the interval  $125 < T < 650^\circ\text{C}$ . In the interval  $650 < T < 937^\circ\text{C}$ , the conductivity goes through a broad, flat maximum; it varies continuously through the transition temperature  $T_t = 937^\circ\text{C}$  and decreases with increasing temperature, as in a metal, above  $937^\circ\text{C}$ . However, all conductivity measurements were made on polycrystalline bars, and the apparent continuity in the conductivity through  $937^\circ\text{C}$  may reflect a high grain-boundary conduction rather than a true continuity of the bulk resistivity.

### III. INTERPRETATION

#### A. General Model

Interpretation of the changes in physical properties, including structure, in the various temperature intervals demarcated by DTA and calorimetric data rests on assumptions about the character of the outer  $d$  electrons and of the cobalt-ion configuration. The general model that we assume is summarized in Table I. The background considerations for this model have already been summarized in the Introduction. In order to justify this model, we must demonstrate that it consistently correlates the various observed physical properties.

#### B. Data Correlation

##### 1. The Interval $-273 < T < 125^\circ\text{C}$

The detailed physical properties and interpretation for this range of temperatures are reported elsewhere<sup>7</sup>

The features of this study that are significant for ideal, bulk LaCoO<sub>3</sub> are (1) the simultaneous existence of high-spin Co<sup>3+</sup> and low-spin Co<sup>III</sup> with an energy separation

$$\epsilon_0 \equiv E_{3+} - E_{\text{III}} \leq 0.08 \text{ eV} \ll \Delta_{cf} \sim 1 \text{ eV} \quad (5)$$

and (2) the most probable space-group symmetry  $R\bar{3}c$ . Equation (5) is obtained from magnetic-susceptibility data and the formula of Griffith<sup>19</sup> relating  $\mu_{\text{eff}}$  to the splitting (including spin-orbit coupling) of the  ${}^1A_1$  low-spin and  ${}^5T_2$  high-spin states. The Griffith formula is the result of a crystal-field calculation and therefore rests on the assumption of localized  $d$  electrons at the Co<sup>3+</sup> ions. This assumption is consistent with other data<sup>1</sup> on transition-metal oxides with perovskite structure, as already discussed in the Introduction. The symmetry assignment  $R\bar{3}c$  means that the cobalt atoms are not distinguishable and therefore that there is no long-range ordering of Co<sup>3+</sup> and Co<sup>III</sup> ions.

Given localized  $d$  electrons, the conductivity  $\sigma = n_g e \mu_n + p_{2g} e \mu_p$  has the form of Eq. (4) because the numbers of mobile charge carriers  $n_g$  and  $p_{2g}$  (the electrons are in orbitals of  $e_g$  symmetry and the holes in orbitals of  $t_{2g}$  symmetry) are

$$n_g = N \exp(-\epsilon/2kT); \quad p_{2g} = N \exp(-\epsilon'/2kT), \quad (6)$$

where  $N$  is the number of cobalt ions per unit volume and

$$\epsilon = \epsilon_0 + \epsilon_g \quad \text{and} \quad \epsilon' = \epsilon_0 + \epsilon_{2g}. \quad (7)$$

The energy  $\epsilon_0$  is defined by Eq. (5);  $\epsilon_g$  and  $\epsilon_{2g}$  are the electrostatic energies associated with the creation of separated divalent and quadrivalent cobalt ions via transfer of an electron or of a hole, respectively. The derivation of this expression has been given, in principle, by Jonker and van Houten.<sup>20</sup> Because the electrostatic energies  $\epsilon_g$  and  $\epsilon_{2g}$  decrease with increasing overlap integrals and  $\Delta^{\pi}_{cac} < \Delta^{\sigma}_{cac}$ , it follows that in an ideally stoichiometric compound

$$\epsilon_g < \epsilon_{2g} \quad \text{and} \quad n_g \geq p_{2g}, \quad (8)$$

even though the total numbers of holes and electrons (trapped plus mobile) are equal.

It is also customary, in a localized-electron model, to use diffusion theory for electron transport and therefore to obtain an activated mobility of the form

$$\mu_{10c} = (eD_0/kT) \exp(-\epsilon_a/kT). \quad (9)$$

For  $d$  electrons in transition-metal oxides the activation energy is usually small ( $\epsilon_a \leq 0.05$  eV). In the vicinity of a localized-electron  $\rightleftharpoons$  collective-electron transition, it may be safely assumed that

$$\epsilon_a < 0.05 \text{ eV} \quad (10)$$

and that it may well vanish at some value of the overlap

integral that is smaller than  $\Delta_e$ . It should not influence significantly the physical properties of LaCoO<sub>3</sub> above room temperature.

## 2. The Interval $125 \leq T < 375^\circ\text{C}$

The  ${}^5T_2$  ground state of an octahedral-site Co<sup>3+</sup> ion is split by spin-orbit coupling into  $J=1, 2, 3$  states, each with a degeneracy  $2J+1$ . The energy  $\epsilon_0$  is the splitting between the  ${}^1A_1$  nondegenerate Co<sup>III</sup> state and the threefold-degenerate  ${}^5T_{2,1}$  state of Co<sup>3+</sup>. The higher multiplets  $J=2, 3$  are separated from the  $J=1$  level by  $2\lambda$  and  $5\lambda$ , respectively, where  $\lambda \approx 400 \text{ cm}^{-1}$ . The temperature  $T_e$  at which the Co<sup>III</sup> and Co<sup>3+</sup> populations are equal is given by

$$\exp(\epsilon_0/kT_e) = 3 + 5 \exp(-2\lambda/kT_e) + 7 \exp(-5\lambda/kT_e)$$

which has the solution  $T_e \approx 420^\circ\text{C}$ . As  $T$  increases toward  $T_e$ , the populations of Co<sup>III</sup> and Co<sup>3+</sup> ions approach one another. Since the radius of a Co<sup>III</sup> ion, which has empty orbitals of  $e_g$  ( $\sigma$ -bonding) symmetry, is significantly smaller than that of a Co<sup>3+</sup> ion, which has half-filled, antibonding orbitals of  $e_g$  symmetry, the oxygen ions between two dissimilar cobalt ions become displaced toward the Co<sup>III</sup> ion and away from the Co<sup>3+</sup> ion. Elastic energy is conserved by a correlation of only Co<sup>III</sup> ions as near neighbors of the high-spin Co<sup>3+</sup> ions.<sup>8</sup> If the Co<sup>3+</sup> population is large, this correlation can only be realized by an ordering of Co<sup>3+</sup> and Co<sup>III</sup> ions on alternate (111) planes, as illustrated by sublattices Co<sub>I</sub> and Co<sub>II</sub> in Fig. 2. Note that this situation calls for the *unusual* possibility of *ordering at higher temperatures*. The fact that  $T_e$  is just above the interval  $125 \leq T < 375^\circ\text{C}$  and that calorimetry shows a higher-order (probably second-order) transition in this interval strongly suggests that this is a temperature range for short-range order. This suggestion is further supported by (a) the symmetry at higher temperatures, (b) the magnetic susceptibility, and (c) the electrical conductivity.

*Symmetry:* The apparent symmetry remains  $R\bar{3}c$  in the interval  $125 \leq T < 375^\circ\text{C}$ , but the Debye-Waller factor is anomalously large and there is considerable uncertainty in the oxygen positions. Above  $375^\circ\text{C}$ , the symmetry  $R\bar{3}$  definitely establishes the existence of long-range ordering of the oxygen-ion displacements.

*Magnetic susceptibility:* Since a cooperative displacement of the oxygen ions in a region of order increases  $\Delta_{cf}$ , thus stabilizing the Co<sup>III</sup> state, on half of the sites, and decreases  $\Delta_{cf}$ , thus tending to stabilize the Co<sup>3+</sup> state, on the other half of the sites, it is clear that the minority population, viz. the Co<sup>3+</sup> population, must increase with increasing order. Therefore the magnetic susceptibility, which is proportional to the number of high-spin Co<sup>3+</sup> ions present, must increase relative to the susceptibility for a disordered phase. This increase is manifest in a decrease in the inverse susceptibility below the values extrapolated from the low-temperature

<sup>19</sup> J. S. Griffith, *Trans. Faraday Soc.* **54**, 1114 (1958), Eq. 17.

<sup>20</sup> G. H. Jonker and S. van Houten, in *Halbleiter Probleme VI*, edited by F. Sauter (Friedrich Vieweg und Sohn, Braunschweig, Germany, 1961), p. 118.

phase (upper dashed line in Fig. 7) and a smaller slope of inverse susceptibility versus temperature above 375°C. Thus the "plateau" in the curve signals a rapid change in the relative populations of high- and low-spin cations as a function of temperature, in direct analogy with the system  $\text{MnAs}_{1-x}\text{P}_x$ <sup>18</sup>, and this population change is consistent with what would be anticipated in a region of increasing short-range order. Once long-range order is established, there is no further discontinuity in the crystalline fields to influence the relative populations, so that the "plateau" in Fig. 7 is confined to the temperature interval of varying amounts of short-range order.

*Electrical conductivity:* An increase in the  $\text{Co}^{3+}$  ion population with increasing order produces a decrease in the effective  $\epsilon_0$  appearing in Eq. (7). From Eq. (6), this means that the onset and increase of short-range order should be accompanied by an abrupt increase in the slope of electrical conductivity versus temperature, which is observed throughout the interval  $125 < T < 375^\circ\text{C}$ .

This effect is further enhanced by the fact that oxygen displacements toward  $\text{Co}^{\text{III}}$  ions and away from  $\text{Co}^{3+}$  ions increase the overlap integrals  $\langle \Delta^{\sigma_{cac}} \rangle$  and  $\langle \Delta^{\pi_{cac}} \rangle$ , so that  $\epsilon_\theta$  and  $\epsilon_{2\theta}$  also decrease. For example, from Eq. (3) the overlap integral between near-neighbor  $\text{Co}^{3+}$  and  $\text{Co}^{\text{III}}$  ions is

$$\langle \Delta^{\sigma_{cac}} \rangle = N \sigma^2 (\lambda_\sigma + \gamma_{\text{I}}) (\lambda_\sigma - \gamma_{\text{II}}) > N \sigma^2 \lambda_\sigma^2, \quad (11)$$

where  $\lambda_\sigma$  is the covalent-mixing parameter for the anion midway between two like cobalt ions,  $(\lambda_\sigma + \gamma_{\text{I}})$  is the mixing parameter for a low-spin cation having the oxygen ion displaced towards it, and  $(\lambda_\sigma - \gamma_{\text{II}})$  is the mixing parameter for the  $\text{Co}^{3+}$  ion having the oxygen ion displaced away from it. Because the overlapping wave functions fall off exponentially from their respective nuclei,

$$\gamma_{\text{I}} - \gamma_{\text{II}} = A \delta_0 + B \delta_0^2 + \dots > 0, \quad (12)$$

where  $\delta_0$  is the oxygen displacement from the center position.

### 3. The Interval $375 \leq T < 937^\circ\text{C}$

The symmetry  $R\bar{3}$  is manifest in this interval not only by a pronounced displacement of the anions toward  $\text{Co}_{\text{I}}$  planes and away from  $\text{Co}_{\text{II}}$  planes, but also where  $400 < T < 650^\circ\text{C}$  by a displacement of the lanthanum ions from the body-center position of the pseudocubic cell. The difference in  $\text{Co}_{\text{I}}\text{-O}$  and  $\text{Co}_{\text{II}}\text{-O}$  separations is nearly 0.5 Å just above 375°C, which is much larger than the total thermal increase in  $a_c$  between room temperature and 1000°C ( $\delta a_c \approx 0.07$  Å). These displacements unambiguously signal a preferential ordering of high- and low-spin cobalt ions at the  $\text{Co}_{\text{II}}$  and  $\text{Co}_{\text{I}}$  sites, respectively. Since the two types of cobalt,  $\text{Co}^{3+}$  and  $\text{Co}^{\text{III}}$ , carry nearly the same effective charge, this ordering must be due to the elastic energies associated with different ionic sizes.

Although the anion displacements are large, nevertheless ordering can only be preferential at these temperatures. Given long-range ordering of the anion displacements so as to create two distinguishable cobalt sublattices,  $\text{Co}_{\text{I}}$  and  $\text{Co}_{\text{II}}$ , there are four primary processes for localized  $d$  electrons that can influence the cobalt-ion configuration on these sublattices and hence the magnitude of the anion displacements that distinguish the sublattices. These are summarized in Table II in the order of increasing energy, or temperature at which they saturate. Two of these processes decrease the ordering of high- and low-spin ions, and two increase it. It is assumed that quadrivalent cobalt, wherever it occurs, is in a low-spin state because of the larger crystal-field splitting associated with the larger cationic charge, and that divalent cobalt is in a high-spin state because of its smaller crystal-field splitting.

The first process describes the fact that long-range order is established where less than 50% of the cobalt atoms are in a high-spin state. This means that just above the ordering temperature, there is some population of low-spin  $\text{Co}^{\text{III}}$  on sublattice  $\text{Co}_{\text{II}}$ . However, as the temperature is further increased, the distribution of  $\text{Co}^{3+}$  and  $\text{Co}^{\text{III}}$  ions between sublattices is enhanced, thus favoring larger anion displacements. This process appears to be dominant in the interval  $375 \leq T < 425^\circ\text{C}$ , since the displacements reach a maximum about 50°C above the short-range-order  $\rightleftharpoons$  long-range-order transition temperature  $T_0 = 375^\circ\text{C}$ .

The second process involves the transfer of an  $e_\theta$  electron from a  $\text{Co}^{3+}$  ion to a  $\text{Co}^{\text{III}}$  ion. Since the great majority of  $\text{Co}^{3+}$  ions are on sublattice  $\text{Co}_{\text{II}}$ , such a transfer creates a net negative charge on sublattice  $\text{Co}_{\text{I}}$  and a positive charge on sublattice  $\text{Co}_{\text{II}}$ . Further, since the rhombohedral angle is  $\alpha_R > 60^\circ$ , this creates an electrical field at the center of the pseudocubic cell that displaces a positive  $\text{La}^{3+}$  ion toward its  $\text{Co}_{\text{I}}$  near-neighbor and away from its  $\text{Co}_{\text{II}}$  near-neighbor along the preferred  $c$  axis (see Fig. 2). Therefore where this process is dominant, finite  $\text{La}^{3+}$ -ion displacements occur. In addition, because quadrivalent cobalt is always low spin and divalent cobalt is always high spin, the electron transfer is always accompanied by an exciton transfer ( $e_\theta$  electron coupled to  $t_{2g}$  hole). Therefore an  $e_\theta$ -electron transfer creates  $\text{Co}^{2+}$  ions on sublattice  $\text{Co}_{\text{I}}$  and  $\text{Co}^{\text{IV}}$  ions on sublattice  $\text{Co}_{\text{II}}$ . This produces a displacement of the anion between them back towards its original position. The  $\text{La}^{3+}$ -ion displacements in the interval  $400 < T < 500^\circ\text{C}$  are accompanied by a continuous decrease in the average anion displacement, which indicates that the second process is dominant in this interval. This is also compatible with the fact that  $\Delta^{\pi_{cac}} < \Delta^{\sigma_{cac}}$ , so that electron transfer via orbitals of  $e_g$  symmetry occurs more readily than that via orbitals of  $t_{2g}$  symmetry (hole transfer).

In the interval  $500 \leq T < 650^\circ\text{C}$ , the  $\text{La}^{3+}$ -ion displacements decrease again to zero, indicating that the difference in charge between sublattices  $\text{Co}_{\text{I}}$  and  $\text{Co}_{\text{II}}$  dis-

TABLE II. Primary processes among localized  $d$  electrons introducing order and disorder into high-temperature  $\text{LaCoO}_3$ .

	Sublattice $\text{Co}_I$	Sublattice $\text{Co}_{II}$	Process	Stabilizes
1	$\text{Co}^{\text{III}}$	$(1-x)\text{Co}^{3+} + x\text{Co}^{\text{III}}$	$x \rightarrow 0$ with increasing $T$	Order
2	$(1-y)\text{Co}^{\text{III}} + y\text{Co}^{3+}$	$(1-y)\text{Co}^{3+} + y\text{Co}^{\text{IV}}$	Electron plus exciton transfer $\text{Co}_{II} \rightarrow \text{Co}_I$	Disorder
3	$(1-z)\text{Co}^{\text{III}} + z\text{Co}^{3+}$	$(1-z)\text{Co}^{3+} + z\text{Co}^{\text{III}}$	Second process plus hole transfer $\text{Co}_{II} \rightarrow \text{Co}_I$ or two-exciton transfer $\text{Co}_{II} \rightarrow \text{Co}_I$	Disorder
4	$(1-\lambda)\text{Co}^{\text{III}} + \lambda\text{Co}^{\text{IV}}$	$(1-\lambda)\text{Co}^{3+} + \lambda\text{Co}^{2+}$ $\text{Co}^{\text{III}}(t_{2g}^6 e_g^0), \text{Co}^{3+}(t_{2g}^4 e_g^2), \text{Co}^{2+}(t_{2g}^5 e_g^2), \text{Co}^{\text{IV}}(t_{2g}^5 e_g^0)$	Hole transfer $\text{Co}_{II} \rightarrow \text{Co}_I$	Order

appears at the higher temperatures. The fact that the anion displacements continue to decrease with increasing temperature throughout this interval indicates that the process responsible for equalizing the charge on the two sublattices is simultaneously creating disorder. Since this is just the requirement for the third process of Table II to be dominant, it is strong evidence for the existence of considerable exciton transfer at higher temperatures. Since  $\Delta^{\sigma_{aac}} < \Delta^{\sigma_{cae}}$ , it is anticipated that hole transfer becomes relatively more important as electron transfer approaches saturation and that initially hole transfer is coupled to electron transfer, which corresponds to exciton transfer. It is to be noted that *exciton transfer occurs because high- and low-spin ions coexist*. Evidence for considerable exciton transfer has already been noted independently in studies of thermal conductivity.<sup>21</sup>

Above 650°C, the anion displacements indicate that greater ordering between low- and high-spin ions is reestablished, but without creating a difference in charge on sublattices  $\text{Co}_I$  and  $\text{Co}_{II}$ . This observation follows from the model, since at higher temperatures both hole and electron transfers become saturated, and independent hole (fourth process) or electron transfers would be equal, thus keeping the sublattice charges equal. Consequently, the  $\text{La}^{3+}$  ions are not displaced and conductivity is nearly temperature-independent. At these temperatures, the total activation energy of Eq. (4) has become

$$q \ll kT.$$

Independent evidence for saturation of the localized charge carriers is found in the electrical conductivity versus temperature, which exhibits a broad maximum just above 650°C.

Furthermore, the fourth process partially reestablishes ordering of low-spin ions on sublattice  $\text{Co}_I$ . However, as the temperature is further increased, electron-configurational entropy tends to destroy the long-range order, and the anion displacements again decrease. The large Debye-Waller factor is consistent with rapidly fluctuating cobalt-ion configurations, and large  $\text{La}^{3+}$ -ion vibrations about the center of the pseudocubic cell.

<sup>21</sup> P. Gerthsen and F. Kettel, J. Phys. Chem. Solids **25**, 1023 (1964).

#### 4. The Interval $T > 937^\circ\text{C}$

The cooperative displacements of both the anions and the lanthanum ions manifest that long-range order is reestablished above 937°C. This is also reflected in the sharp drop of the Debye-Waller factor. The fact that band-electron correlations, in contrast to localized-electron correlations, are long-range strongly suggests that long-range order has been reestablished via the transformation of localized  $e_g$  orbitals into collective  $\sigma^*$ -band orbitals at  $T_t = 937^\circ\text{C}$ . Since  $\Delta^{\sigma_{aac}} < \Delta^{\sigma_{cae}} \approx \Delta_e$ , it follows that orbitals of  $t_{2g}$  symmetry would remain localized, thereby still providing the distinction between two kinds of cobalt. With ideal long-range order, the  $\text{Co}_I$  sublattice contains cobalt atoms with outer configuration  $t_{2g}^{6-x}\sigma^{*y}$  and the  $\text{Co}_{II}$  sublattice  $t_{2g}^{4+x}\sigma^{*2-y}$ , where  $x < y$ , the fraction  $\delta = y - x$  representing the transfer of electronic charge from sublattice  $\text{Co}_{II}$  to sublattice  $\text{Co}_I$ . Although  $\sigma^*$ -band electrons belong collectively to all the cobalt atoms, the difference in potential between sublattice  $\text{Co}_{II}$  and sublattice  $\text{Co}_I$  keeps  $y$  a fraction and  $\delta$  a small fraction, so that the ions on sublattices  $\text{Co}_I$  and  $\text{Co}_{II}$  remain high- and low-spin, respectively. However,  $\delta$  does represent a partial disproportionation of the cobalt-ion charge that creates an electric field at the body-center position of the pseudocubic cell. Although the rhombohedral angle is  $\alpha_R = 60.0^\circ$  above 937°C, nevertheless the anion displacements define a unique axis and the positive lanthanum ions are shifted along this axis away from the  $\text{Co}_{II}$  sublattice, which has a larger positive charge than the  $\text{Co}_I$  sublattice. As the band broadens,  $\delta$  increases to simultaneously increase the  $\text{La}^{3+}$ -ion displacements and decrease the anion displacements.

The fact that the conductivity decreases with increasing temperature, as in a metal, is also compatible with  $\sigma^*$ -band formation above  $T_t$ .

#### 5. The Character of the Transition at $T_t$

Differential thermal analysis has established that the transition at 937°C is first order and endothermic. Since the heat of transformation is positive and is proportional to the entropy change,

$$\Delta H = T_t \Delta S, \quad (13)$$

it follows that the total entropy change

$$\Delta S = \Delta S_{\text{config}} + \Delta S_{\text{vib}} + \Delta S_{\text{el}} > 0 \quad (14)$$

must be positive on increasing the temperature through  $T_t$ . The first two terms in Eq. (14) represent the configurational and vibrational entropies of the nuclei plus core electrons; the last term represents the entropy of the outer electrons.

The fact that there is no change in the symmetry  $R\bar{3}$  on passing through the transition suggests that

$$\Delta S_{\text{config}} \approx 0, \quad (15)$$

any configurational entropy associated with static displacements of the lanthanum being relatively small. On the other hand, the large drop in the Debye-Waller factor at  $T_t$  shows that

$$\Delta S_{\text{vib}} < 0 \quad (16)$$

is relatively large. It is concluded that

$$\Delta S_{\text{config}} + \Delta S_{\text{vib}} < 0. \quad (17)$$

Combination of Eqs. (14) and (17) gives

$$\Delta S_{\text{el}} > 0 \quad (18)$$

as the driving force for the first-order phase change. This conclusion is the strongest evidence for a localized-electron  $\rightleftharpoons$  collective-electron phase change at  $T_t$ , and it implies that there is a significant latent heat associated with the formation of collective electrons and their associated Fermi surface. This means that crystal-field theory, which rests on the assumption of localized electrons, and band theory, which describes a Fermi gas in a periodic potential, apply to two distinct thermodynamic states of the electrons.

If this reasoning is correct, then it follows from our discussion in the Introduction that  $\Delta\sigma_{\text{cac}}$  should not be so decreased by the thermal expansion of the lattice that  $\Delta H$  is too large, where  $\Delta H$  is the heat of transformation that is required to make  $\Delta\sigma_{\text{cac}} > \Delta\epsilon$ . This condition appears to be fulfilled in  $\text{LaCoO}_3$ . First, note that the pseudocubic cell edge  $a_c$  increases by only  $\delta a_c \approx 0.07$  Å between room temperature and  $1000^\circ\text{C}$  and is essentially continuous through the transition temperature  $T_t$ . Second, the anion displacements just above  $T_t$  are large compared with  $\delta a_c$ , so that

$$\langle \Delta\sigma_{\text{cac}} \rangle_{T_t} \geq \langle \Delta\sigma_{\text{cac}} \rangle_{20^\circ\text{C}} \quad (19)$$

although it may be somewhat smaller than  $\langle \Delta\sigma_{\text{cac}} \rangle_{500^\circ\text{C}}$ .

Given our conclusion that a first-order localized-electron  $\rightleftharpoons$  collective-electron transition takes place at  $T_t$ , it is surprising that the electrical conductivity varies continuously through the transition. This surprise is not only due to the fact that discontinuities in electrical conductivity are usually associated with first-order phase changes, but also because Mott,<sup>22</sup> who first discussed the possibility of a sharp transition between

localized and collective electrons, applied the concept to impurity-band formation in semiconductors to account for the dramatic changes in low-temperature conductivity that occur with small changes in impurity concentration. Indeed this bias subsequently led him to suggest that the semiconducting  $\rightleftharpoons$  metallic transitions observed in compounds like  $\text{V}_2\text{O}_3$  and  $\text{VO}_2$  were of this type, whereas we now know that these transitions are better described by a narrow-band Jahn-Teller effect.<sup>23,24</sup> The reason for the discontinuous changes in conductivity that are observed in these transitions, and in the usual first-order transitions, is that changes in bonding produce changes in the number of charge carriers. In  $\text{LaCoO}_3$ , the number of charge carriers is fixed by the number of  $\text{Co}^{3+}$  ions present, which approaches 50% at high temperatures and is not appreciably changed through the transition. So long as the width of the  $\sigma^*$ -band energies is  $\Delta\epsilon \leq kT_t \approx 0.1$  eV, all of the  $\sigma^*$ -band electrons are charge carriers. Similarly, below  $T_t$  where the maximum in the conductivity indicates  $q < kT$ , where  $q$  is defined by Eq. (4), saturation of the charge carriers has been reached. Therefore the number of charge carriers is unchanged by the transition from localized to collective electrons.

However, the conductivity is also proportional to the charge-carrier mobility, which has the form of Eq. (9) for localized electrons and the form

$$\mu_{\text{coll}} = e\tau/m^* \quad (20)$$

for collective electrons. The temptation is to assume that if the localized and collective descriptions correspond to two different electronic states, then there must be a discontinuity in the mobility on going from one phase to the other. This assumption, although never explicit in Mott's qualitative argument, is readily inferred to provide a major contribution to the changes in electrical conductivity that are found where impurity-band formation occurs. However, *charge-carrier mobility is independent of the existence of a Fermi surface*, so there is no *a priori* requirement that the charge-carrier mobility should not vary continuously through a localized-electron  $\rightleftharpoons$  collective-electron transition, provided only that  $\epsilon_a \ll kT$  at  $T_t$ . Therefore, the fact that the conductivity varies continuously through  $T_t = 937^\circ\text{C}$  in  $\text{LaCoO}_3$  is interpreted to mean that *the mobility is continuous through the transition, and probably all physical properties that are independent of the existence of a Fermi surface are continuous through a localized-electron  $\rightleftharpoons$  collective-electron transition.*

Since electrical conductivity measurements were made on polycrystalline bars, it is perhaps dangerous to assume that the bulk conductivity is continuous through  $T_t$ . In fact, the discontinuous drop in the Debye-Waller factor through  $T_t$  suggests that the creation

<sup>23</sup> J. B. Goodenough, Phys. Rev. **117**, 1442 (1960); Colloque International sur des Dérives Semi-métalliques, University of Paris, 1965 (to be published).

<sup>24</sup> D. Adler, Bull. Am. Phys. Soc. **11**, 261 (1966).

<sup>22</sup> N. F. Mott, Can. J. Phys. **34**, 1356 (1956).

of a Fermi surface enhances selected vibrational modes at the expense of others, in which case the mobility could be indirectly dependent upon the creation of a Fermi surface. However, any discontinuity in the mobility appears to be small.

#### IV. CONCLUSION

Structural, calorimetric, magnetic, electrical-conductivity, and thermal-conductivity data are not only consistent with the model of Table I for  $\text{LaCoO}_3$ , but appear to require it. This model, though complicated, rests on only three physical assertions:

(1) Crystal-field splitting and intra-atomic-exchange splitting are of nearly the same energy for trivalent cobalt in the octahedral interstices of a perovskite structure, which means that at finite temperatures high-spin  $\text{Co}^{3+}$  ions coexist with low-spin  $\text{Co}^{\text{III}}$  ions and that  $\text{Co}^{2+}$  ions are high-spin, and  $\text{Co}^{\text{IV}}$  ions are low-spin.

(2) In the perovskite structure, the elastic energies associated with ions of different radii are strong enough to correlate low-spin ions as near-neighbors of a high-spin ion (and vice versa), which means that preferential ordering of low- and high-spin ions occurs at higher temperatures, where the two species coexist in nearly equal numbers.

(3) For  $3d$ -transition-metal oxides with perovskite structure, covalent mixing of anion orbitals with the

$3d$  orbitals is strong enough to cause  $\sigma^*$ -band formation ( $\Delta\sigma_{eac} > \Delta_c$ ) if the ions are low-spin (net atomic spin is  $S=0, \frac{1}{2}$  for  $\text{Co}^{\text{III}}$  and  $\text{Co}^{\text{IV}}$ ), but is weak enough to leave the crystal-field  $3d$  orbitals localized ( $\Delta\sigma_{eac} < \Delta_c$ ) if the ions are high-spin ( $S=2, \frac{3}{2}$  for  $\text{Co}^{2+}$  and  $\text{Co}^{3+}$ ). However, where high-spin and low-spin ions coexist, then  $\langle \Delta\sigma_{eac} \rangle \approx \Delta_c$ .

Independent studies have established the first<sup>3-8,25</sup> and the last<sup>1</sup> of these assertions, and the second, which was anticipated earlier,<sup>8</sup> is confirmed by the symmetry of  $\text{LaCoO}_3$  which has been established in this study.

There are three significant pieces of information that follow from the model of Table I and the physical data:

(1) Crystal-field theory and band theory describe two different thermodynamic states of the electrons, and the entropy of the collective (band) electrons is larger so that a localized-electron  $\rightleftharpoons$  collective-electron transition is first order.

(2) Where low- and high-spin ions coexist, exciton transport is an important process.

(3) Electron mobility and, by inference, other physical properties that are independent of the existence of a Fermi surface vary *continuously* through a first-order localized-electron  $\rightleftharpoons$  collective-electron transition, provided the crystal symmetry is also continuous through the transition and the volume change is negligible.

#### APPENDIX

Relative integrated intensities have been measured on a sample of  $\text{LaAlO}_3$  prepared by usual ceramic techniques. Powder data were collected on the setup described above. Refinement of the structure indicated

TABLE III. Experimental and calculated intensities for  $\text{LaAlO}_3$ .

$h$	$k$	$l$	$2\theta$	Experimental intensities (Normalized to sum of obs. or calc. intensities)	Calculated intensities	$h$	$k$	$l$	$2\theta$	Experimental intensities (Normalized to sum of obs. or calc. intensities)	Calculated intensities
1	0	0	20.28	0	1	2	-1	-1	59.70		
1	1	1	20.32			0	1	3	59.74	1468	1472
						2	3	3	59.83		
1	0	1	23.47	1775	1736	3	0	0	63.75		
0	-1	1	33.40	3702	3747	-2	1	-2	63.75		
2	1	1	33.45			3	0	2	63.78	0	2
						3	1	3	63.83		
1	-1	-1	39.39			3	3	3	63.89		
0	1	2	39.41			0	-2	2	70.17		
1	2	2	39.46	0	9	4	2	2	70.29	757	738
						-2	2	1	73.90		
2	0	0	41.23			3	1	-1	73.92	0	4
2	2	2	41.31	1579	1547	4	2	1	73.99		
						4	3	2	74.05		
2	0	2	48.00	1319	1302	-3	1	0	75.13		
0	-1	2	52.58			3	3	0	75.19		
3	1	1	52.63	0	2	4	1	1	75.19	395	404
3	2	2	52.68			4	3	3	75.31		
						3	2	-1	80.00	669	633
1	-1	2	54.06	800	801	4	3	1	80.09		
3	1	2	54.13								

<sup>25</sup> G. Blasse, J. Appl. Phys. **36**, 879 (1965).

TABLE IV. Experimental and calculated intensities for LaCoO<sub>3</sub> at 400°C;  $R\bar{3}$  space group.

$h$	$k$	$l$	$2\theta$	Experimental intensities (Normalized to sum of obs. or calc. intensities)	Calculated intensities	$h$	$k$	$l$	$2\theta$	Experimental intensities (Normalized to sum of obs. or calc. intensities)	Calculated intensities
Hexagonal						Hexagonal					
-1	0	2	23.10	946	930	3	0	0	58.40		
1	1	0	32.72	7593	7593	2	1	4	58.44	2828	2851
1	0	4	33.05			3	-1	4	59.11		
						-1	0	8			
2	0	2	40.38	1226	1260	2	2	0	68.38		
0	0	6	41.96			2	0	8	69.16	1013	1139
-2	0	4	47.13	2283	2216	3	0	6	73.70	296	129
						-3	0	6			
1	2	2	52.82			1	3	4	78.06		
3	-2	2		484	567	4	-3	4			
1	1	6	53.31			1	2	8	78.52	1244	1196
-1	-1	6				3	-2	8			
						4	0	4	87.14	256	289

that the space group  $R\bar{3}c$  is more probable than  $R\bar{3}m$  or  $R\bar{3}$ , and the value of the distortion parameter  $\alpha$  in the hexagonal basis was found to be identical to that reported by neutron-diffraction measurements,<sup>15</sup> viz.,  $\alpha=0.475$ . The fitting of the data is shown in Table III.

Table IV presents a typical LaCoO<sub>3</sub> run. The temperature was 400°C and the  $R$  factor is 3.3% on the intensities.

## Shape of the $F$ -Aggregate Bands in KCl and KBr. I. Measurement

ROGER W. WARREN

*Westinghouse Research Laboratories, Pittsburgh, Pennsylvania*

(Received 29 September 1966)

Measurements are reported on the shape of the  $R_1$ ,  $R_2$ ,  $M$ ,  $N_1$ , and  $N_2$  bands in KCl and KBr from 10 to 300°K. The first three moments are determined for the  $M$  band, and the peak position and half-width are determined for the remaining bands.

### INTRODUCTION

THE  $F$  center in KCl has remained of interest to theoretical and experimental investigators for a very long time. It is the prototype of a large class of centers, found in many materials, that differ from impurity centers by the absence of a single positive core to which the electrons are bound. From observations of the absorption and emission bands of the  $F$  center and their dependence upon temperature and other parameters such as stress, one hopes to gain knowledge about the wave functions of the electrons, the static and vibrational structure of the lattice, and the coupling between the  $F$  center and the lattice. One of the most direct experimental techniques has been to measure the shape of the absorption band as a function of temperature.<sup>1</sup> The theories which are used to analyze

such measurements are discussed in various review articles.<sup>2</sup>

It appears, however, that the  $F$  center may not be the ideal center upon which to spend one's efforts, for it is not as simple a defect as one at first supposes. There are various experimental observations which illustrate this. The fluorescent lifetime of the  $F$  center, for instance, is unusually long<sup>3</sup> and the  $F$  band in the cesium halides is split into several resolvable components.<sup>4</sup> Many complications such as these can be related to the electronic degeneracy of the excited state of the  $F$  center. A better center for many purposes, then, would be one involving only nondegenerate electronic levels.

<sup>2</sup> C. C. Klick and J. H. Schulman, in *Solid State Physics*, edited by F. Seitz and D. Turnbull (Academic Press Inc., New York, 1957), Vol. 5, p. 97; J. H. Schulman and W. D. Compton, *Color Centers in Solids* (The MacMillan Company, New York, 1962), p. 69.

<sup>3</sup> R. K. Swank and F. C. Brown, *Phys. Rev. Letters* **8**, 10 (1962).

<sup>4</sup> P. R. Moran, *Phys. Rev.* **137**, A1016 (1965).

<sup>1</sup> J. D. Konitzer and J. J. Markham, *J. Chem. Phys.* **32**, 843 (1960).